Technical University of Denmark

DTU

Performance Evaluation of a SOA-based Rack-To-Rack Switch for Optical Interconnects Exploiting NRZ-DPSK

Karinou, Fotini; Borkowski, Robert; Prince, Kamau ; Roudas, I.; Tafur Monroy, Idelfonso ; Vlachos, K.

DTU Library
Technical Information Center of Denmark

Performance Evaluation of a SOA-based Rack-To-Rack Switch for Optical Interconnects Exploiting NRZ-DPSK

F. Karinou[(1),(2)], R. Borkowski[(2)], K. Prince[(2)], I. Roudas[(1)], I. Tafur Monroy[(2)], and K. Vlachos[(3)]

[(1)] Dept. of Electrical & Computer Engineering, University of Patras, Rio 26504, Greece; E-mail:
   karinou@ece.upatras.gr
[(2)] DTU Fotonik, Dept. of Photonics Eng., Technical University of Denmark, Ørsteds Plads, Building
   343, DK-2800 Kgs. Lyngby, Denmark
[(3)] Dept. of Computer Engineering & Informatics, University of Patras, Rio 26504, Greece

Abstract *We experimentally study the transmission performance of 10-Gb/s NRZ-DPSK through concatenated AWG MUX/DMUXs and SOAs employed in an optimized 64×64 optical supercomputer interconnect architecture. NRZ-DPSK offers 9-dB higher dynamic range compared to conventional IM/DD.*

Introduction

Data traffic in high-performance computing (HPC) systems is continuously increasing in volume and a larger number of modules (i.e., boards, drawers, racks, etc.) need to be interconnected using point-to-point links with bandwidths in the order of several GHz[1]. Given this increasing need for capacity, optics is the most promising solution for serial or parallel interconnects longer than a few meters at Gb/s data rates[2]. Their cost-effectiveness and practicality are already demonstrated[3] in active optical cables composed of vertical-cavity surface emitting lasers (VCSELs)[4] and multi-mode fibers (MMFs). Additionally, in order to minimize the overall power consumption high-sensitivity modulation formats are explored[5,6].

The Optical Shared MemOry Supercomputer Interconnect System (OSMOSIS) project proposed an optical packet switch architecture[7] for rack-to-rack interconnection in HPC systems. It is a two-stage, broadcast-and-select, 64×64 optical interconnect, which uses semiconductor optical amplifiers (SOAs), acting as on-off gates, to perform switching. In the past[8], we examined the impact of SOA transmission impairments on the performance of two versions of the OSMOSIS switch fabric, an SOA-rich one, originally proposed[7], and its optimized version, with minimal active component count[9], assuming 10-Gb/s intensity-modulation/direct-detection (IM/DD) links. In a different study[5], we explored the more futuristic scenario of using coherent polarization division multiplexed (PDM) quadrature phase shift keying (QPSK) to reduce the impact of SOA nonlinearities in the aforementioned optical switch fabric. In this paper, we consider a more realistic short-term solution, i.e., using non-return-to-zero (NRZ) differential phase shift keying (DPSK) with balanced direct detection in the OSMOSIS switch fabric. Using balanced detection, DPSK has a 3-dB sensitivity advantage compared to IM/DD[10]. Moreover, DPSK is more resilient to SOA nonlinearities[11] than conventional IM/DD due to its envelope constancy[12]. In particular, we experimentally investigate, for the first time, the performance of 10 Gb/s NRZ-DPSK format in the 64×64 OSMOSIS switch fabric. It is shown that NRZ-DPSK channels experience up to 1 dB OSNR penalty when transmitted through the 64×64 OSMOSIS switch compared to the back-to-back case. At the same time, NRZ-DPSK outperforms by 9 dB IM/DD regarding the dynamic range. Given the above NRZ-DPSK constitutes a possible candidate for next-generation optical interconnects.

Experimental setup

Fig. 1 shows the experimental setup. There are 64 transmitters partitioned into four sets[8]. The transmitters of each set are assigned 16 equidistant carrier frequencies (the allocation is shown in Fig. 2, where λ_0=1546.897 nm). The 16 carrier frequencies are grouped into four wavebands in sets of four, occupying an aggregate bandwidth of 2.7 THz. Guard bands facilitate waveband multiplexing/demultiplexing. The channel spacing within a waveband is $\Delta f = 100$ GHz. In the experimental setup, eight lasers (shown with solid lines in Fig. 2), representing the first two wavebands of the optimized OSMOSIS switch fabric architecture[8], are multiplexed with an arrayed waveguide grating (AWG) and, subsequently, they are modulated using a 10 Gb/s pseudo-random binary sequence (PRBS), to form eight identical NRZ-DPSK WDM signals. Semiconductor lasers in the two remaining wavebands W_3-W_4, i.e., λ_{16}-λ_{27} (shown with dashed lines in Fig. 2) are not
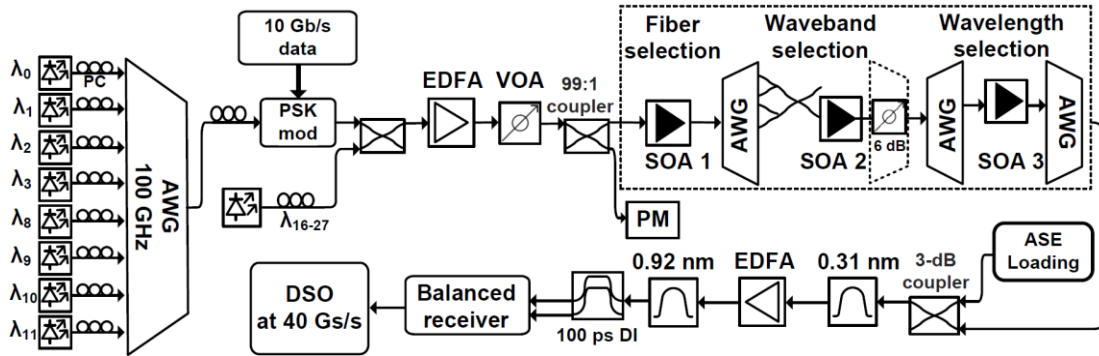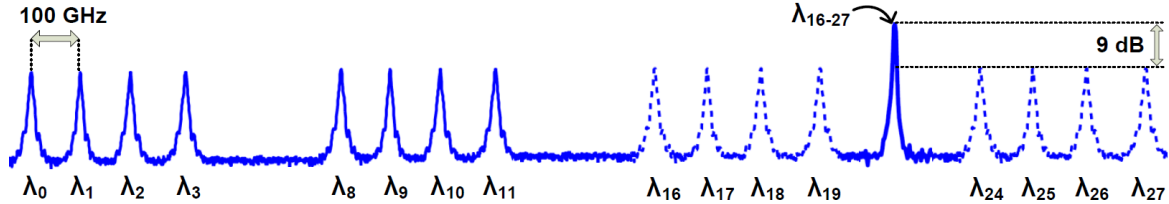
Fig. 1: Experimental setup.

Fig. 2: Original (λ$_0$-λ$_{27}$) and implemented (blue solid line) wavelength allocation scheme.

available in the lab. They are emulated by another continuous wave (CW) laser source placed between W$_3$-W$_4$ (see Fig. 2), with eight times the nominal power of a single channel (Fig. 2). All signals are combined through a coupler and then the WDM signal is amplified by an erbium-doped fiber amplifier (EDFA) and attenuated by a variable optical attenuator (VOA), representing the 1:64 star coupler of the actual OSMOSIS switch fabric architecture[7]. A 99:1 coupler is used to monitor the input power into the first SOA, which is optimized so that the SOAs work in the linear regime. Next, the signals pass through three consecutive wavelength selection stages employing SOAs as on-off gates. The three SOAs used in the experiment are 1-mm long, with a 3-dB bandwidth of 90 nm, a small-signal gain of 15 dB, a high input saturation power of approximately 4 dBm, and a low polarization dependent gain (PDG) of <0.2 dB. The SOA device and its characteristics (Gain vs P$_{in}$ and P$_{out}$ vs P$_{in}$, in blue and in green, respectively), is shown in Fig. 3. The first SOA is used to select the desired fiber. The waveband selection stage should ideally consist of a pair of 400-GHz bandwidth AWGs interconnected with four SOAs, acting as on-off gates. In our experiment, due to lack of resources, it consists of a 100-GHz AWG MUX with interconnected arms to emulate the 400-GHz AWG required in the proposed architecture[9], a second SOA, and an attenuator of 6 dB to emulate another 400-GHz AWG MUX, not available in the lab. The selection of the desired channel is performed via a third wavelength selection stage, which is comprised of a pair of conventional AWG MUX/DMUX, with 100 GHz spacing, and a
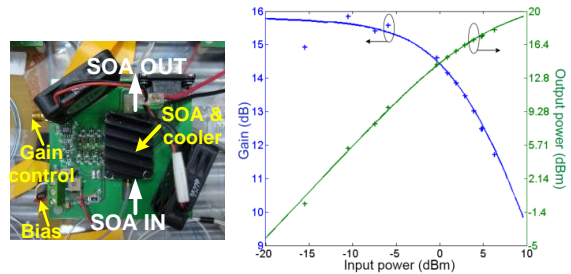

Fig. 3: SOA device used in the experimental setup.

single SOA. Amplified spontaneous emission (ASE) noise is loaded after the last selection stage, in order to adjust the delivered OSNR to the receiver. Then, the selected wavelength is filtered by a 0.31-nm bandwidth optical filter, amplified by an EDFA, and filtered again by a 0.92-nm bandwidth optical filter to reject out of band noise stemming from the optical preamplifier. For direct-detection of DPSK signals, a 100-ps delay interferometer (DI) was employed in front of a balanced receiver. The photocurrent is sampled using a digital sampling oscilloscope (DSO) at 40 Gsamples/s and bit error rate (BER) measurements are carried out to investigate the performance of the switch.

Results and Discussion

BER measurements as a function of the optical signal-to-noise ratio (OSNR) are performed in the following cases: i) back-to-back, i.e., when the selection stages of the OSMOSIS optical switch fabric in Fig. 1 are omitted; and ii) aftet transmission through the optical switch fabric. The results are shown in Fig. 4. The performance of all DPSK implemented channels is approximately the same, since the OSNR spread of the curves is around 1 dB at BER=1×10^{-3}. No significant penalty is observed
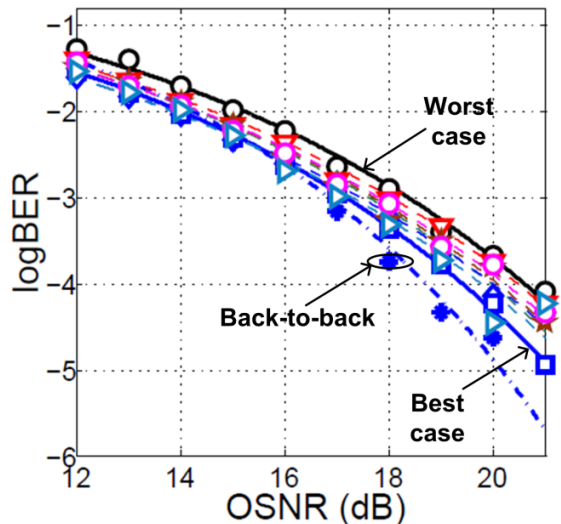
Fig. 4: BER vs OSNR (RB=0.1 nm) for the eight implemented wavelengths. Experimental data are fitted with exponential curves.
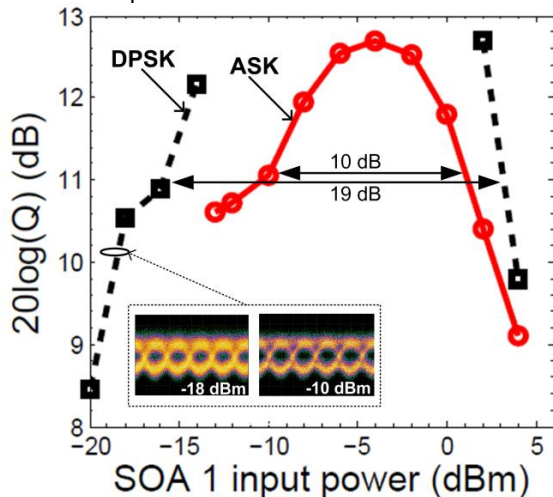

Fig. 5: Q-factor vs SOA 1 input power for DPSK and IM/DD modulation formats. Eye diagrams for P$_{in}$=-10 dBm and -18 dBm in the DPSK case are shown as insets.
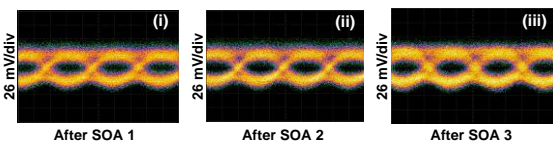

Fig. 6: Experimental eye diagrams after each consecutive selection stage of the optimized OSMOSIS architecture.

between the back-to-back case and the best channel (λ_8), while 1 dB OSNR penalty is measured for the worst channel (λ_0).

To test the robustness of DPSK to SOA nonlinearities, we measured the BER for channel λ_0 at various input powers into the first SOA. The results are shown in Fig. 5 (black squares) and are compared with the corresponding measurements using the ASK format (red circles). ASK results are obtained using the experimental setup described in a

previous work[8]. Taking as an arbitrary reference Q=11 dB (corresponding to BER $\cong$ 2×10^{-4}), DPSK proves to outperform ASK by 9 dB in terms of the dynamic range of the received signal. As dynamic range we define the power range at the first SOA for which the the Q-factor remains above 11 dB. Discontinuities in the DPSK black curve indicate error-free transmission at these input power values.

To illustrate the impact of concatenated SOAs on the performance of the optical switch fabric using DPSK, representative eye diagrams are shown in Fig. 6 (i)-(iii) after the fiber, the waveband and the wavelength selection stage of the switch architecture, respectively. We observe that the eye opening does not degrade significantly as the number of the selection stages increase.

Conclusions

We evaluated the performance of NRZ DPSK and demonstrated its superiority compared to IM/DD in an optimized 64×64 optical interconnect architecture that uses SOAs to perform optical packet switching. We experimentally investigated its performance using 10 Gb/s optical links. All NRZ-DPSK channels experience approximately the same performance while NRZ-DPSK outperforms IM/DD by 9 dB in terms of the dynamic range of the input signal power to the first SOA. DPSK is an appealing candidate for next-generation optical interconnects, likely to substitute IM/DD, due to its low implementation complexity and equipment cost.

Acknowledgements

References

1. H.Liu et al., Proc. 18th Symp. on HPI (2010).
2. C. L. Schow et al., Proc. OFC'08, OMK5 (2008).
3. http://www.lanl.gov/roadrunner/
4. R. Johnson et al, Proc. CLEO'08, CPDB2 (2008).
5. F. Karinou et al., Proc. OFC'10, JWA62 (2010).
6. M. Glick et al., Proc. ICTON'09, WeB23 (2009).
7. R. Hemenway et al., JON **3**, 900 (2004).
8. F. Karinou et al., JLT **29**, 3167 (2011).
9. I. Roudas et al., Proc. LEOS'07, ThG3 (2007).
10. A.H. Gnauck et al., JLT **23**, 115 (2005).
11. P. S. Cho et al., PTL **16**, 918 (2004).
12. X. Wei et al., PTL **16**, 1582 (2004)